International Journal of Applied Engineering Research ISSN 0973-4562 Volume 13, Number 3 (2018) pp. 1768-1775

Evaluation of Laser-Sintered CR-CO and TI Alloys for Dental Applications

Lucia Denti

Department of Engineering, University of Modena and Reggio Emilia, "Enzo Ferrari", via Vivarelli 10, Modena 41125, Italy.

Abstract

Even if additive layer manufacturing techniques have been introduced in industries since last '80, the application in medicine is quite recent and tend to remain at research level. In dental implantology the introduction of these technologies in the prostheses production could introduce more precision well time and money savings. Dental prostheses may be built by additive layer manufacturing, specifically by direct metal laser sintering (DMLS). The target of this paper is to investigate the mechanical and microstructural characteristics, comparing samples built along different orientation. Tensile specimens were built in accordance with ASTM E8M both by DMLS (EOSINT-M270), using Cr-Co alloy and Ti6Al4V alloy. An experimental plan was designed to evaluate the effect of different built orientation. Density, hardness, tensile performances, rupture surfaces SEM observation, porosity evaluation and microstructure observation were performed on the following group of specimens (4 specimen for each group): were produced (4 for each group) in three orientations with respect to the machine distinctive directions

Both alloys have good mechanical performance in terms of tensile strength, elongation and hardness. The specimens revealed a low porosity and of consequence to be quite fully densified. The microstructure observed is very fine and explain the mechanical characteristics of the materials.

The statistic analysis doesn't evidence a unique difference between the different building orientation. DMLS produce parts with excellent mechanical properties independently from building orientation.

INTRODUCTION

Additive manufacturing (AM) techniques permit the production of objects with complex geometry from the tridimensional CAD model (Computer Aided Design) without tools. The basic idea is to think every object as consisting of many layers with a thin thickness (up to 0.05 mm). The part is then made with progressive addition of material, section by section, hence the methodology AM was named. These technologies were introduced in industry in '80 to realize models and prototypes, but nowadays the progress has lead to the possibility to directly realize the final object. There are many AM techniques that use different materials: polymer, metal or sand [1-4]. The great potential and good evolution of techniques lead to introduce additive layer manufacturing in medicine, in fact the field of prostheses and medical restorations is characterized by the need of products that are customized for each patient, with a high degree of personalization [5]. AM techniques have been used for the construction of prosthesis [6], such as mandible reconstruction or crown [7,8]. They are usefull also for planning operation through the construction of surgical guides [6,9].

This paper focus on maxillo-facial surgery, in particular implantology.

Implantology is a field under continuous innovation, where there is research on finding new materials, new components, new fabrication processes to improve the duration, the aesthetics and the functionality of implants obtaining a better quality of life for patients. For example gold crowns have replaced with metal-ceramic or ceramic crowns [10-12]. AM technologies could be used in the construction of metal-ceramic fixed partial dentures (FPDs). The construction of the metallic part of these prostheses involve a large series of manual operation of the dental technician, and the result is often to ascribe to his ability. Introducing additive layer manufacturing for metal prosthesis fabrication, the process could acquire more repeatability and predictability respect to traditional technique [13]. The Direct Metal Laser Sintering (DMLS) produce parts with metallic powder, such as cr-co and Ti alloys. During the process, a thin layer of powder is deposited in the building camera with a coater or roll, starting from a feed containers. In a next step, a laser melts the powder entirely creating a cross section of the final product. Then a piston lowers and a further thin layer of powder is deposited and the process is repeated till the end. DMLS enables the formation of cavities and undercuts which, with conventional methods, cannot be produced or can be produced with great difficulty. The most complex geometries parts are built layer by layer, directly from CAD model, fully automatically, in only few hours and without tooling[1,2]. The combined action of advantages deriving from the application of additive layer manufacturing processes translates into good savings in money and delivery times.The DMLS technique for dental application has the potentiality to substitute the traditional technique. On the other hand the DMLS process is quite complex and a large number of factors are involved to obtain a good result [14], and even if some author have investigated this process [14-17], the literature data are little and not completed. In particular, it has not been studied if the building direction in the plane of construction affect the mechanical performance. It is very important to investigate this particular point of the process because the complete prostheses develop along an arc and not in a straight direction, so it would be parts weaker than other with the consequence to have a rupture.

This paper investigate the mechanical and microstructural properties of two dental alloy built by DMLS, confronting,

through statistic methods, samples built in different orientation.

MATERIAL AND METHODS

Tensile specimens were produced, following ASTM E8M specifications for flat unmachined specimens from powder metallurgy. Figure 1 and table 1 show the main dimensions.

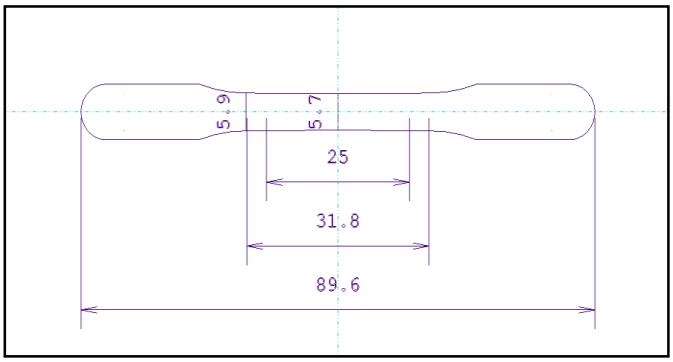

Figure 1. Tensile specimens.

Table 1: Main dimensions of tensile specimens (ASTM E8M).

Gage length (mm)	25.0
Length of reduced section (mm)	31.8
Overall length (mm)	89.6
Width at center (mm)	5.7
Width at the end of reduced sec. (mm)	5.9
Thickness (mm)	3.6

Parts were produced by Direct Metal Laser Sintering (DMLS) using Ti6Al4V grade 5 and a Co-Cr-Mo alloy: the alloys composition are shown in table 2, while mechanical performances of bulk material are shown in table 3

Table 2:

ALLOY	**WEIGHT PERCENTAGE [%]**						
Cr-Co	Co	Cr	Mo	Si	Mn	Altri	
	59.5	31.5	5.0	2.0	1.0	1.0	
Ti6Al4V	Ti	Al	V	C	Fe	N	O
	88 -90.2	5.5-6.7	3.5-4.5	<0.08	<0.25	<0.25	<0.2

Table 3:

MECHANICAL PROPRIETY	**Ti6Al4V**	**Cr-Co**
MELTING POINT [±15°C]	1634 – 1664	1240 – 1348
DENSITY[kg/dm^3]	4.43	8.8
TENSILE STRENGHT σ_{max} [Mpa]	938	960

Standard parameters were used on EOSINT-M270 to fabricate the laser-sintered specimens (table 4).

Table 4: Parameters used for building the DMLS specimens

PARAMETERS	
laser power	200W
laser spot diameter	0.200 mm
Scan speed	up to 7.0 m/s
Building speed	2-20 mm3/s
Layer thickness	0.020 mm
Protective atmosphere	max 1.5% oxigen

The machine uses a Yb-fibre laser. Every layer is built with the following strategy: the slice area is divided into squares of 4 mm side, built one next to the other. After every square's building the laser spot is realigned. On each layer the laser acts with parallel wipes directed according to a definite scan vector. For the next layer the scan vector is rotated by 25° with respect to the previous one. Figure 2 shows a scheme of the building strategy

Specimens in both the alloys were produced (4 for each group) in three orientations with respect to the machine distinctive directions:

- "0" group: specimens' axis parallel to the X direction in the machine building volume
- "90" group: specimens' axis parallel to the Y direction in the machine building volume
- "45" group: specimens' axis parallel to the bisector of the X-Y quadrant

Density of the specimens was measured using the Archimede's principle and compared to the theoretical one for each alloy to estimate parts residual porosity. UTS tests were performed using an elongation speed of 5mm/min, on SCHENK (HYDROPULS PSB) testing machine, with a load cell acting up to 250 kN. Results were elaborated through statistical tools and the presence of significant differences between the groups was assessed by the t-test with a level of significance of 0.05.

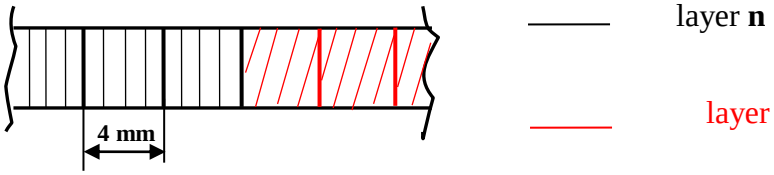

Figure 2: Laser scanning strategy

After testing, rupture surfaces were observed using the scanning electron microscope (SEM) to investigate failure mechanisms and joining phenomena between the particles. It was chosen to observe the surface rupture of a sample for each type of process, choosing a sample that showed characteristics of tensile strength close to the average recorded for that group.

The specimen was also observed at the optical microscope (OM) to calculate data related to porosity. Several micrographs for each magnification were acquired through a CCD camera, made binary and analyzed through a software tool for image analysis to obtain:

- Percentage porosity, calculated as the area fraction of pores out of the overall area;
- The average size of pores

To observe the sections at SEM and OM, the specimens were cut with a metallurgical microcutting, then embedded in a metallurgical epoxide resin and polished till a fine grinding. Final polishing was carried out with a plan cloth and a 1 μm diamond suspension. The surfaces of one specimen for each group was metallographically prepared with diamond past up to 1 μm and then, after etching, they were investigated by optical microscope. The Dix-Keller etchant (HF 2% vol, HCl 1,5 % vol, HNO3 2,5 % vol; water bal.) was used for the Ti6Al4V while for the Co-Cr-Mo alloy a electrochemical etching (HCl 0,1 M, 2V, 2 min.). Hardness test has been chosen following ISO 4498 standard (Sintered metal materials, excluding hardmetals - Determination of apparent hardness and microhardness) In particular, Rockwell C hardness has been performed following the specific standard ISO 6508 (Rockwell hardness test), with five test on each sample.

RESULTS AND DISCUSSION

Density

Results are shown in table 5, where the first row shows the theoretical alloy density for comparison. Density values show an extremely narrow scattering and residual porosity is below 0.2% for Cr-Co samples and 0.02% for Titanium samples. In both cases a nearly full density was achieved.

Table 5: Specimens density

Theoretical alloy density [kg/dm^3]					
Ti6Al4V	4.43		**CoCr**	8.8	
	MEASURED DENSITY [kg/dm^3]			**MEASURED DENSITY [kg/dm^3]**	
	MEAN	**SD**		**MEAN**	**SD**
Ti 0	4.43	0.003	**CoCr 0**	8.60	0.01
Ti 45	4.41	0.020	**CoCr 45**	8.61	0.01
Ti 90	4.40	0.020	**CoCr 90**	8.60	0.06

Table 6: Hardness of specimens

	HRC	
	MEAN	ST.DEV.
Ti 0	**39.8**	2.58
Ti 45	**38.7**	3.85
Ti 90	**38.9**	2.53
CoCr 0	**46.9**	1.13
CoCr 45	**46.9**	0.93
CoCr 90	**47.0**	0.76

Table 7: P value of t-test performed on hardness results

Ti 0° vs. Ti 45°	0.29
Ti 0° vs. Ti 90°	0.26
Ti 45° vs. Ti 90°	0.86
CrCo 0° vs. CrCo 45°	0.76
CrCo 0° vs. CrCo 90°	0.91
CrCo 45° vs. CrCo 90°	0.62

Hardness

Titanium samples proved to have a HRC of near 39, and Cr-Co specimens have a hardness of 47. T-test performed (table VII) on results indicate that there aren't significant difference between each group, then the orientation doesn't have an influence on hardness.

Tensile Test

The specimens have been subjected to tensile strength test following E8 standard, Results are showed in table 8 . As to Ti samples, one specimen of "90" group and one of "0" group were excluded from the results because of technical problems during the test, for another specimen of "90" group elongation was excluded because of slipping. The same happened for one specimen of "90" group and one of "45" group among CoCr parts. UTS results are shown in table 8.

Table 8: Results for ultimate tensile strength and elongation at break.

	UTS [MPa]		ε_b[%]	
	MEAN	ST.DEV.	MEAN	ST.DEV.
Ti64 0	**1110**	0.57	**12.43**	11.7
Ti64 45	**1098**	26.11	**12.60**	0.65
Ti64 90	**1080**	6.08	-	-
CoCr 0	**1281**	12.80	**12.81**	0.45
CoCr 45	**1290**	7.91	**14.09**	0.22
CoCr 90	**1301**	7.64	**13.00**	0.72

Mean UTS of titanium specimens resulted in the range 1080-1110 MPa, with elongations of about 12.5%. All groups proved to have good test repeatability with a very low standard deviation.Regarding tensile strength, there is a significant difference between group "0" and group "90", even if the difference is of about 30 MPa, as visible in figure 3a . Considering elongation instead, there are not significant differences between the groups, as can be appreciated in figure 3b .

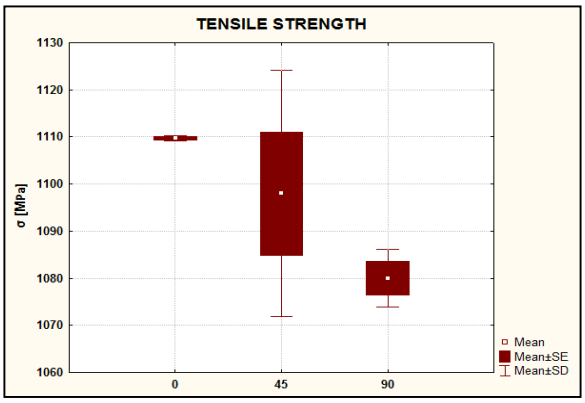

(a)

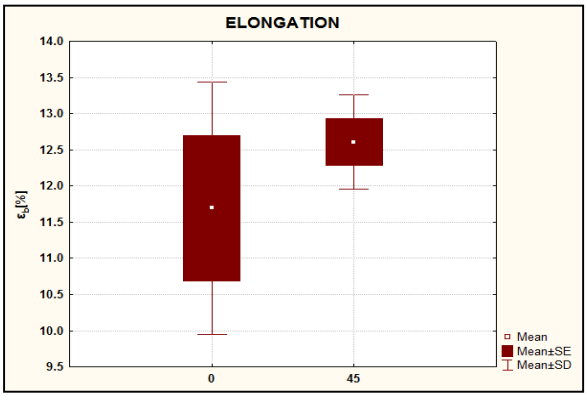

(b)

Figure 3a and 3b: Box and whiskers diagram showing UTS and elongation for the three groups of Ti specimens

As to CoCr parts, mean UTS was about 1280-1300 MPa, with elongations in the range 12.8 to 14%. All groups proved to have good test repeatability with a very low standard deviation. Regarding tensile strength, there are not significant differences between the groups if a significance of 95% is assumed, but a light increase can be noticed from "0" to "45" and "90" groups, as visible in figure 4a. The t-test on UTS between "0" and "90" groups provides a p-value of 0.06, only slightly above the adopted confidence level.

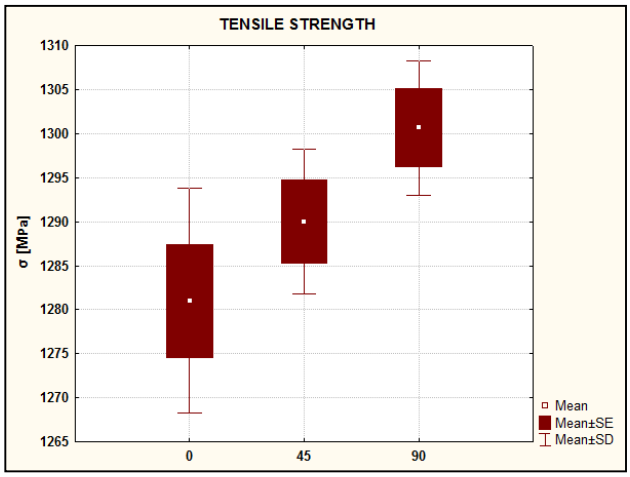

(a)

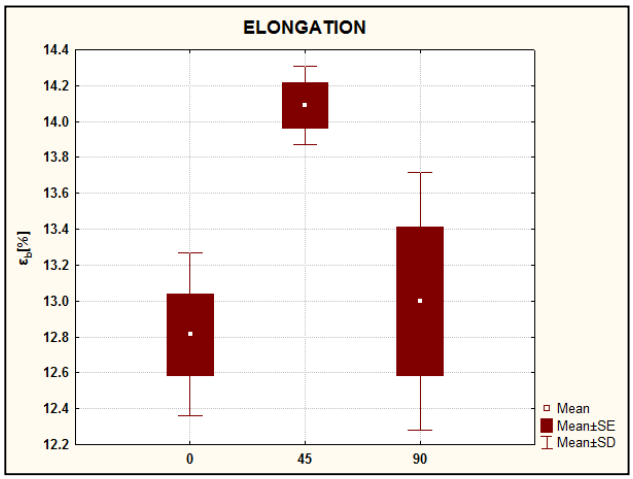

(b)

Figure 4a and 4b: Box and whiskers diagram showing UTS and elongation for the three groups of CoCr specimens

Considering elongation instead, there are significant differences between "45" group and the other two directions, as can be appreciated in figure 4b.

SEM observation of rupture surface

For Ti specimens failure occurs by a variety of mechanisms that can be observed on macro views of the rupture surfaces, as the one in Figure 5. If the different building orientations are compared, different rupture morphologies can be perceived in

the macroscale, but observations of the micromechanisms are in effect equal in all the samples. This a typical fracture of ductile materials, usually named to cup and cone fracture. This form of ductile fracture occurs in stages that initiate after necking begins. First, small microvoids form in the interior of the material. Next, deformation continues and the microvoids enlarge to form a crack. In figure 5a is visible a planar zone that is the last who break, in figure 5b there in a migrograph of this zone and can be appreciated the presence of dimples. The described aspects are common to specimens produced in all the considered orientations. Overall, observations on the rupture surfaces suggest an extremely fine grain structure, which will be verified though observations on polished etched sections.

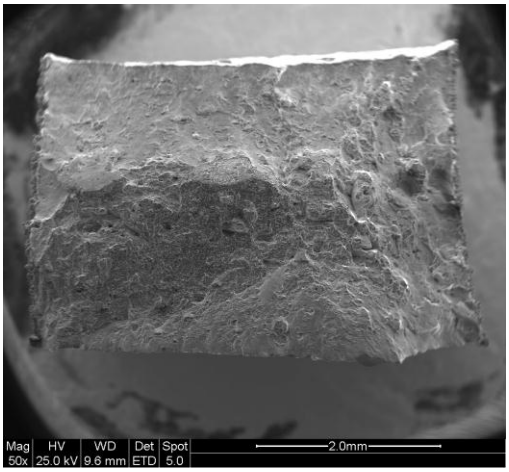

(a)

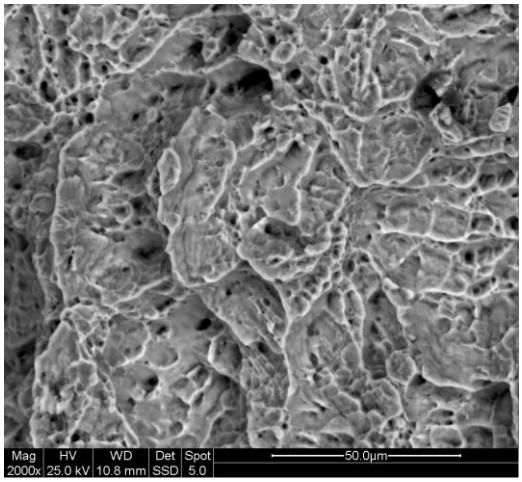

(b)

Figure 5a and 5b. Macro view and micrograph of a Ti specimen rupture surface.

Some cavities can be noticed on the rupture surfaces (Figure 5c), whose formation occurred during layer construction and indicated a balling phenomena [18]

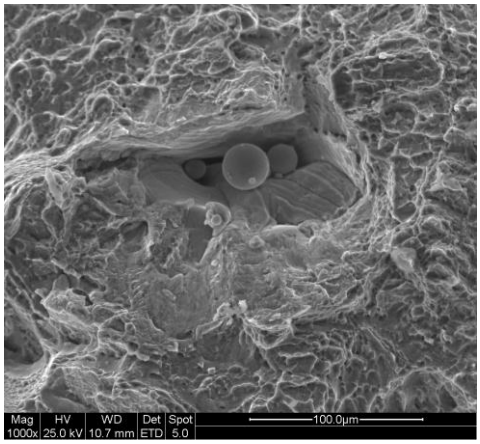

Figure 5c. Cavity on the rupture surface of a "0" specimen.

The rupture surface of CrCo specimens shows a uniform morphology across the section, shown in figures 6 . Failure seems to occur mainly by cleavage, even if the values of elongation at break would suggest a more ductile mode. In this cases can be used the term "quasi-cleavage", that indicate a fracture that has various amounts of transgranular cleavage but with evidence of plastic deformation.

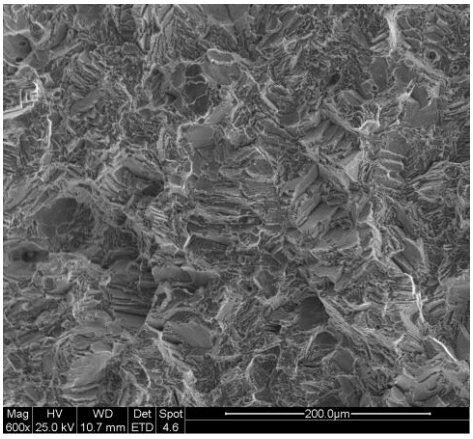

(a)

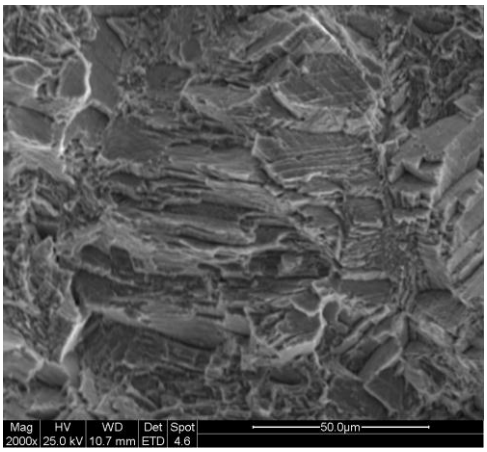

(b)

Figure 6a and 6b . Morphology of the rupture surface of Cr-Co specimens.

Observing the DMLS specimens it can be noticed that the different layers are no more visible, this indicates that the particles are strongly joined together not only within each layer but also between different layers. Isotropy in the build direction is a rarity in additive layer manufacturing techniques.

Porosity

Table 8 shows the results of the porosity calculation in the sections of the different specimens. In a preliminary phase samples were observed as a whole to assess the possibility of share the same in different areas, calculating for each of them porosity. The specimens revealed homogeneity.

Table 9: Porosity measured on specimens

SAMPLE	AVERAGE SIZE[μm²] Mean (dev. st.)	AREA FRACTION [%] Mean (dev. st.)
Ti 0	4.58 (6.092)	0.04 (0.074)
Ti 45	2.04 (0.552)	0.21 (0.064)
Ti 90	17.60 (11.318)	0.28 (0.225)
CoCr 0	15.87 (29.687)	0.55 (0.655)
CoCr 45	10.09 (8.856)	0.30 (0.214)
CoCr 90	18.78 (25.938)	0.43 (0.453)

The titanium specimens present a rather uniform porosity with an average size of pores contained, between 4 and 18 μm² and a low porosity that in under 0.3%. The t-test indicated that there is a significant difference in porosity due to orientation between Ti 0 and the others, but in percentage term the difference is contained in value of 0.2%.

The Cr-co specimen present a porosity that varies from 0.3% to near 0.55%, with an mean average size of pores between 10 and 20 μm². The t-test indicated that there is not a significant difference in porosity due to orientation

Table 10: p-value obtained by t-test on porosity results

	AVERAGE SIZE	POROSITY
Titanio 0° vs. Titanio 45°	0,26	0,00
Titanio 0° vs. Titanio 90°	0,01	0,01
Titanio 45° vs. Titanio 90°	0,00	0,46
Cromo 0° vs. Cromo 45°	0,61	0,32
Cromo 0° vs. Cromo 90°	0,84	0,66
Cromo 45° vs. Cromo 90°	0,38	0,49

Microstructure

The analysis of microstructure of titanium samples revealed that the tree orientation doesn't present difference. The specimen is homogeneous and exhibits the acicular α′ martensite microstructure, wich forms where the cooling rate is hight. In fact a rapid quenching leads to a martensitic transformation, leading to a very fine needle-like microstructure [19]. This kind of microstructure is difficult to obtain industrially and for this reason is not common

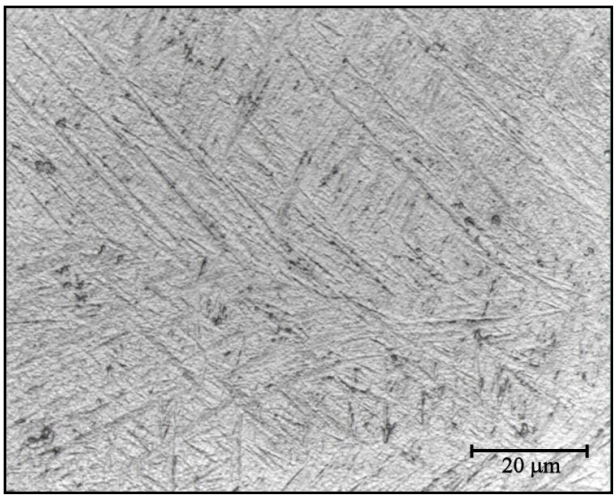

Figure 7: Micrograph of microstructure of Ti specimens

The Cr-co Specimens present a very particular macro-structure, like "fish scales", where the boundary are due to the melted zone by the laser. In fact all the semicircles are oriented in the same direction, that is growing one. Higher magnification shows a very fine acicular microstructure, where grain are oriented in different ways. The grains have a diameter lower than 1 μm as is visible in figure 8c and 8d. This fine structure is responsible of the performance of the material that are higher than those expected from bulk material.

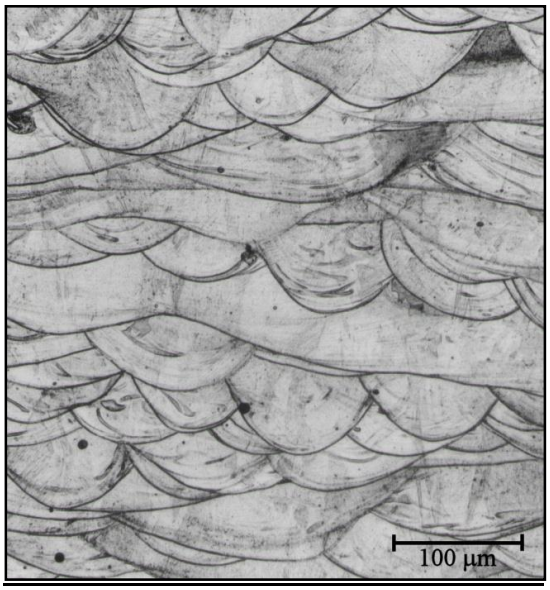

(a)

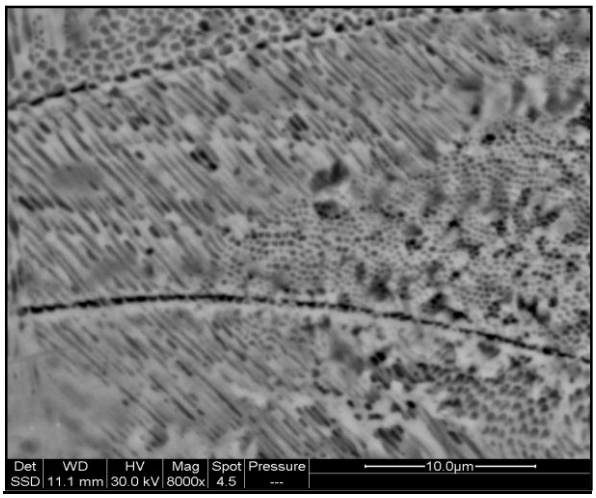

(b)

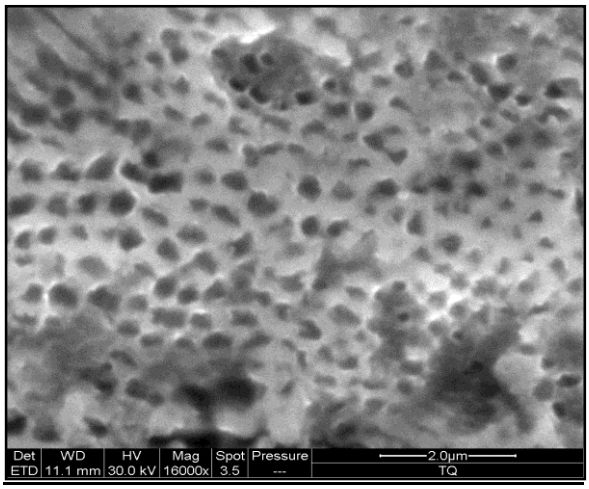

(c)

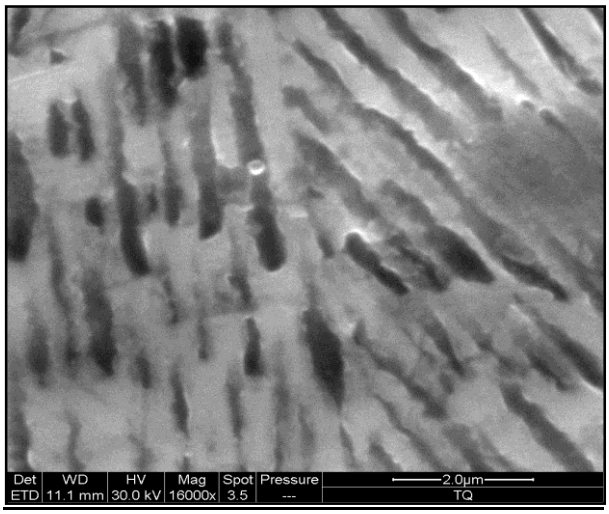

(d)

Figure 8a, 8b, 8c, 8d: Micrograph of microstructure of Cr-Co specimens

CONCLUSION

DMLS technique has been investigated comparing specimens built in different orientation in building camera, with two different dental alloy: Cr-Co and Ti6Al4V. Mechanical, physical, chemical and microstructural properties have been compared.

Both alloy produced by DMLS show high tensile strength, low porosity and high hardness. The physical and mechanical properties of the material mainly depend on its microstructure, so the observed very fine microstructure cause the macroscopic performances of the specimens. The microstructure of titanium specimens is a particular α' martensitic structure, whereas the Cr-Co show grain of the order of micrometers.

The statistic test does not indicate a unique difference between the building orientations, confronting all the results there are significant difference between group only in few cases and in these cases the numerical difference is very contained, as 30 MPa on 1100 MPa.

DMLS process is very reliable and repeatable; the experimental results show a very low standard deviation.

It can be concluded that, as to the possibility of using DMLS technology for the realization of prostheses in Cr-Co and Ti6Al4V alloy, from a mechanical point of view, the DMLS technique has good performance that does not depend from the orientation in the building camera.

REFERENCES

[1] Ashley S, "Rapid Prototyping is Coming of Age," Mechanical Engineering July 1995: 63

[2] Ashley S, "From CAD Art to Rapid Metal Tools," Mechanical Engineering March 1997: 82

[3] Bassoli E, Gatto A, Iuliano L. Joining mechanisms and mechanical properties of PA composites obtained by Selective Laser Sintering. RAPID PROTOTYPING JOURNAL, 2012 vol. 18 (2), p. 100-108

[4] Bassoli E, Gatto A, Iuliano L, Violante MG. 3D Printing technique applied to Rapid Casting.Rapid Prototyping Journal, 2007 vol. 13(3), p. 148-155,

[5] Glantz PO, Ryge G, Jendresen MD, Nilner K. Quality of extensive fixed prosthodontics after five years. J Prosthet Dent 1984;52:475-9.

[6] Walton TR. An up to 15-year longitudinal study of 515 metal-ceramic FPDs: Part 1. Outcome. Int J Prosthodont 2002;15:439-45.

[7] Laurell L, Lundgren D, Falk H, Hugoson A. Long-term prognosis of extensive polyunit cantilevered fixed partial dentures. J Prosthet Dent 1991;66:545-52.

[8] Eliasson A, Arnelund CF, Johansson A. A clinical evaluation of cobalt-chromium metal-ceramic fixed partial dentures and crowns: A three- to seven-year retrospective study. J Prosthet Dent. 2007 Jul;98(1):6-16.

[9] Tan K, Pjetursson BE, Lang NP, Chan ES. A systematic review of the survival and complication rates of fixed partial dentures (FPDs) after an observation period of at least 5 years. Clin Oral Implants Res 2004;15:654-66.

[10] Schmalz G, Garhammer P. Biological interactions of dental cast alloys with oral tissues.Dent Mater 2002;18:396-406.

[11] Al-Hiyasat AS, Bashabsheh OM , Darmani H. An investigation of the cytotoxic effects of dental casting alloys. Int J Prosthodont 2003;16:8-12.

[12] Andersson M, Oden A. A new all ceramic crown. A dense-sintered, high purity alumina comping with porcelain. Acta Odontol Scand 1993;51:59-64

[13] Richard Bibb, Dominic Eggbeer, Robert Williams, Rapid manufacture of removable partial denture frameworks, Rapid Prototyping Journal Volume: 12 Issue: 2 2006

[14] Maarten van Elsen, Farid Al-Bender, Jean-Pierre Kruth, (2008) "Application of dimensional analysis to selective laser melting", Rapid Prototyping Journal, Vol. 14 Iss: 1, pp.15 – 22

[15] Simchi A, Direct laser sintering of metal powders: Mechanism, kinetics and microstructural features Original Materials Science and Engineering: A, Volume 428, Issues 1-2, 25 July 2006, Pages 148-158

[16] Facchini L, Magalini E, Robotti P, Molinari A, Höges S, Wissenbach K, Ductility of a Ti-6Al-4V alloy produced by selective laser melting of prealloyed powders, Rapid Prototyping Journal Volume: 16 Issue: 6 2010

[17] Kruth, J.-P.; Mercelis, P.; Van Vaerenbergh, J.; Froyen, L.; Rombouts, M., Binding Mechanisms in Selective Laser Sintering and Selective Laser Melting, 2005, Rapid prototyping journal, Vol. 11, p.26-36

[18] Dongdong Gu, Yifu Shen, Balling phenomena in direct laser sintering of stainless steel powder: Metallurgical mechanisms and control methods, Materials & Design, Volume 30, Issue 8, September 2009, Pages 2903-2910

[19] H. Matsumoto, H. Yoneda, K. Sato, S. Kurosu, E. Maire, D. Fabregue, T. J. Konno, A. Chiba, Room-temperature ductility of Ti–6Al–4V alloy with α' martensite microstructure, Materials Science and Engineering A, Volume 528, Issue 3, 25 January 2011, Pages 1512-1520